

NASA/TM—1999-209060



# Rate Dependent Deformation and Strength Analysis of Polymer Matrix Composites

Robert K. Goldberg  
Glenn Research Center, Cleveland, Ohio

Donald C. Stouffer  
University of Cincinnati, Cincinnati, Ohio

---

March 1999

## The NASA STI Program Office . . . in Profile

Since its founding, NASA has been dedicated to the advancement of aeronautics and space science. The NASA Scientific and Technical Information (STI) Program Office plays a key part in helping NASA maintain this important role.

The NASA STI Program Office is operated by Langley Research Center, the Lead Center for NASA's scientific and technical information. The NASA STI Program Office provides access to the NASA STI Database, the largest collection of aeronautical and space science STI in the world. The Program Office is also NASA's institutional mechanism for disseminating the results of its research and development activities. These results are published by NASA in the NASA STI Report Series, which includes the following report types:

- **TECHNICAL PUBLICATION.** Reports of completed research or a major significant phase of research that present the results of NASA programs and include extensive data or theoretical analysis. Includes compilations of significant scientific and technical data and information deemed to be of continuing reference value. NASA's counterpart of peer-reviewed formal professional papers but has less stringent limitations on manuscript length and extent of graphic presentations.
- **TECHNICAL MEMORANDUM.** Scientific and technical findings that are preliminary or of specialized interest, e.g., quick release reports, working papers, and bibliographies that contain minimal annotation. Does not contain extensive analysis.
- **CONTRACTOR REPORT.** Scientific and technical findings by NASA-sponsored contractors and grantees.

- **CONFERENCE PUBLICATION.** Collected papers from scientific and technical conferences, symposia, seminars, or other meetings sponsored or cosponsored by NASA.
- **SPECIAL PUBLICATION.** Scientific, technical, or historical information from NASA programs, projects, and missions, often concerned with subjects having substantial public interest.
- **TECHNICAL TRANSLATION.** English-language translations of foreign scientific and technical material pertinent to NASA's mission.

Specialized services that complement the STI Program Office's diverse offerings include creating custom thesauri, building customized data bases, organizing and publishing research results . . . even providing videos.

For more information about the NASA STI Program Office, see the following:

- Access the NASA STI Program Home Page at <http://www.sti.nasa.gov>
- E-mail your question via the Internet to [help@sti.nasa.gov](mailto:help@sti.nasa.gov)
- Fax your question to the NASA Access Help Desk at (301) 621-0134
- Telephone the NASA Access Help Desk at (301) 621-0390
- Write to:  
NASA Access Help Desk  
NASA Center for Aerospace Information  
7121 Standard Drive  
Hanover, MD 21076

NASA/TM—1999-209060



# Rate Dependent Deformation and Strength Analysis of Polymer Matrix Composites

Robert K. Goldberg  
Glenn Research Center, Cleveland, Ohio

Donald C. Stouffer  
University of Cincinnati, Cincinnati, Ohio

National Aeronautics and  
Space Administration

Glenn Research Center

---

March 1999

## Acknowledgments

The authors would like to acknowledge Fiberite, Inc. for providing the material used for the experimental tests on the IM7/977-2 system along with additional information and data. The authors would also like to acknowledge Cincinnati Testing Laboratories, Inc. for conducting the tensile tests on the IM7/977-2 material presented in this report.

Trade names or manufacturers' names are used in this report for identification only. This usage does not constitute an official endorsement, either expressed or implied, by the National Aeronautics and Space Administration.

Available from

NASA Center for Aerospace Information  
7121 Standard Drive  
Hanover, MD 21076  
Price Code: A03

National Technical Information Service  
5285 Port Royal Road  
Springfield, VA 22100  
Price Code: A03

# Rate Dependent Deformation and Strength Analysis of Polymer Matrix Composites

Robert K. Goldberg  
National Aeronautics and Space Administration  
Glenn Research Center  
Cleveland, Ohio 44135

and

Donald C. Stouffer  
University of Cincinnati  
Cincinnati, Ohio 45221

## SUMMARY

A research program is being undertaken to develop rate dependent deformation and failure models for the analysis of polymer matrix composite materials. In previous work in this program, strain-rate dependent inelastic constitutive equations used to analyze polymers have been implemented into a mechanics of materials based composite micromechanics method. In the current work, modifications to the micromechanics model have been implemented to improve the calculation of the effective inelastic strain. Additionally, modifications to the polymer constitutive model are discussed in which pressure dependence is incorporated into the equations in order to improve the calculation of constituent and composite shear stresses. The Hashin failure criterion is implemented into the analysis method to allow for the calculation of ply level failure stresses. The deformation response and failure stresses for two representative uniaxial polymer matrix composites, IM7/977-2 and AS4-PEEK, are predicted for varying strain rates and fiber orientations. The predicted results compare favorably to experimentally obtained values.

## LIST OF SYMBOLS

$D_o$	inelastic material constant representing maximum inelastic strain rate
$E$	elastic modulus of material
$G$	shear modulus of material
$J_2$	second invariant of deviatoric stress tensor
$K_{ij}$	components of $K_2$ effective stress
$k_f$	fiber volume ratio of composite
$n$	inelastic material constant representing rate dependence of material
$q$	inelastic material constant representing hardening rate of material
$S_{ij}$	deviatoric stress components
$S$	ply shear strength
$X_T$	ply longitudinal tensile strength
$X_C$	ply longitudinal compressive strength
$Y_T$	ply transverse tensile strength

$Y_C$	ply transverse compressive strength
$Z_o$	material constant representing initial isotropic hardness of material
$\alpha$	scaling factor for shear components of $K_2$ effective stress
$\beta$	material constant used in scaling shear components of $K_2$ effective stress
$\epsilon_{ij}$	strain tensor components
$\epsilon_{ij}^I$	inelastic strain components
$\epsilon_e^I$	effective inelastic strain
$\gamma_{ij}$	engineering shear strain components
$\Omega_{ij}$	back stress component
$\Omega_m$	inelastic material constant representing value of back stress at saturation
$\sigma_{ij}$	stress tensor components
$\sigma_m$	mean or hydrostatic stress
•	quantities with dots above them represent rates

### Subscripts

Af	bottom left subcell of composite unit cell (fiber material)
Am	bottom right subcell of composite unit cell (matrix material)
B1	top left subcell of composite unit cell (matrix material)
B2	top right subcell of composite unit cell (matrix material)
R1	region of composite unit cell consisting of subcells Af and Am
R2	region of composite unit cell consisting of subcells B1 and B2
f	fiber related material property
m	matrix related material property
12	in-plane shear stress or strain components
11,22,33	normal stress or strain components

## INTRODUCTION

NASA Glenn Research Center has an ongoing research program to investigate the feasibility of developing hardwall fan containment systems composed of polymer matrix composite materials for aircraft engines. In such an application, the composite would be loaded at strain rates up to several hundred per second. To design a composite containment system, the ability to correctly predict the deformation and failure behavior of the composite under the high rate loading condition is required.

In previous reports [1,2], a strain-rate dependent inelastic constitutive model was described which was utilized to simulate the deformation response of two polymers, Fiberite 977-2 and PEEK. The implementation of the constitutive equations into a mechanics of materials based composite micromechanics model was also discussed. Micromechanics models are utilized to predict the effective deformation response of a composite material based on the properties and response of the individual constituents. The deformation response of two uniaxial polymer composites reinforced with carbon fibers, IM7/977-2 and AS4/PEEK, was predicted using the developed analysis technique for various fiber orientations and strain rates. The predicted values compared favorably

to experimentally obtained results. Both the nonlinearity and rate dependence of the stress-strain curves were captured in the analysis. Only relatively low strain rates were examined due to the availability of experimental data. However, the techniques can be extended to high strain rate conditions. Furthermore, only unidirectional composites with arbitrary fiber orientation angles are currently being analyzed. A laminate theory has not been implemented into the model.

Using the methodology as described in [1] and [2], the stresses and deformations in the composite were reasonably well predicted in general. However, for fiber orientation angles in which shear stresses in the matrix are dominant, the match between experimental and predicted values was not as good. These results suggested that the shear stresses in the matrix were not being predicted correctly. The discrepancies were determined to primarily be a function of two parameters. First, the mathematical formulation used to compute the effective inelastic strain for the composite was found to be incorrect. Second, the polymer constitutive model discussed in [1] appeared to predict the shear stresses incorrectly, and required modification. In particular, the shear terms in the polymer flow law were determined to be a function of the hydrostatic pressure, which was not accounted for in the original equations. Both of these modifications to the original model will be discussed in this report.

In order to develop structural level failure and penetration models, ply level failure needs to be accurately predicted. In this work, the Hashin [3] failure model will be implemented in order to predict ply level failure for a variety of fiber orientation angles. An advantage of a ply failure model of this type is that even though the criterion is based on macroscopic stresses, the model predicts failure based on constituent level failure mechanisms using a phenomenological approach.

This report begins with a background section. First, a review of the literature discusses the effects of the hydrostatic pressure on the inelastic response of polymers. Next, previous investigations into developing ply level failure models for polymer matrix composites will be presented.

After the background section, the modifications to the computation of the effective inelastic strain in the micromechanics technique will be presented. In the previous work [2], a simple volume averaging of the inelastic strain in each material region was utilized to compute the effective inelastic strain. As will be discussed in this report, this approach was modified in a manner such that the assumptions implied in the original micromechanics model are accounted for more accurately.

Next, the modifications that were implemented into the polymer constitutive equations will be discussed. The original model will be given, and the modifications to the shear terms in the inelastic flow law that were implemented will be presented. The deformation response of two representative uniaxial polymer matrix composites will be predicted and compared to experimental values for a variety of fiber orientation angles and strain rates.

Finally, the ply level failure model that was implemented will be discussed. The details of the model will be presented. The ply level failure stresses for the chosen representative composites will be predicted for a variety of fiber orientations and strain rates and compared to experimental values.

## BACKGROUND

### Pressure Dependence of Polymer Inelastic Deformation

The hydrostatic stress state has been found to have a significant effect on the yield behavior of a polymer [4-7]. Increasing the hydrostatic pressure has been found to increase the yield stress [4-6]. The effect of hydrostatic pressure also results in the tensile and compressive yield stresses of a polymer being unequal. This effect can be incorporated in the Maximum Shear Stress (Tresca) and Maximum Distortion Energy (von Mises) yield theories to develop yield criteria that can be applied to polymers [7]. In the Maximum Shear Stress criteria, the shear yield stress is a linear function of the hydrostatic stress. In the Maximum Distortion Energy criteria, the octahedral shear stress at yield is a linear function of the mean stress. Ward [4-6] also incorporated these concepts into modifying the Eyring based yield criteria, in which the hydrostatic pressure is incorporated as an additional term in the equations relating the octahedral shear strain at yield to the octahedral shear stress at yield.

If the pressure dependence is to be incorporated into an inelastic state variable constitutive model, appropriate effective stress definitions need to be defined. Bordonaro [8] attempted several such modifications. One such modification involved utilizing total stresses instead of stress deviators in the effective stress definition. Another such modification consisted of adding in a multiple of the mean stress to the product of stress deviators. Neither of these modifications yielded acceptable results when compared to experimental data for materials such as Nylon and PEEK, indicating that an alternative effective stress definition is required.

### Ply Level Composite Failure Models

As indicated in reviews such as those conducted by Nahas [9], many failure criteria exist to predict the ply level ultimate strength in polymer matrix composites. No one criterion has been found to be superior for all materials and loading conditions. Several "classic" criteria are in use, as detailed in texts such as those by Gibson [10] and Herakovich [11], and in review papers such as those by Reddy and Pandey [12]. Simple models such as the Maximum Stress and Maximum Strain criteria simply compare the stresses (or strains) in each coordinate direction to the ultimate values. The drawback to these models is that stress interaction is not accounted for to any significant extent. In the Tsai-Hill criteria, a quadratic combination of stresses and strengths in each coordinate direction is compared to a failure value. In this model, stress interaction is accounted for, but differences between tensile and compressive strengths are not considered. The Tsai-Wu criterion utilizes a tensor based failure criterion, which allows for differences between tensile and compressive failure strengths. In general, the more sophisticated

failure criteria such as Tsai-Hill or Tsai-Wu provide improved failure predictions than simple models such as Maximum Stress or Maximum Strain, but studies like that conducted by Sun and Quinn [13] show that this is not always the case.

In all of the models discussed above, composite failure is considered on purely a macroscopic level, with no attention being paid to the specific mechanisms which cause failure. In reality, failure in a composite is a result of specific local mechanisms such as tensile fiber failure, matrix cracking or delamination [14]. While accurate modeling of these local failure mechanisms would require a detailed micromechanical analysis, several researchers have developed phenomenological failure criteria that predict local failure mechanisms based on macroscopic stresses.

Hashin [3] developed a failure model that predicts fiber failure or matrix failure (tensile or compressive) based on appropriate quadratic combinations of stresses and failure strengths. Chang and co-workers [15-17] developed similar quadratic failure criteria, but also accounted for nonlinearities in the stress-strain curve by using integrals of strain energy in the shear terms instead of shear stresses and shear strengths. Yen [18] extended the Chang criteria from a plane stress assumption to a fully three-dimensional model. He then utilized the modified criteria to predict composite damage and failure for a transient dynamic impact application. Banerjee [19] also successfully utilized the Hashin and Chang failure criteria to predict damage and failure for a polymer matrix composite subject to impact loads. Rotem [20] developed a quadratic failure criteria based on local failure mechanisms, but in the matrix failure equations the matrix failure strength and matrix stress were used along with the macroscopic stress and strength values. Tabiei et al. [21] utilized the Hashin criterion to predict the failure of a polymer matrix composite with nonlinearities in the stress-strain curve, but accounted for the nonlinearities in the composite constitutive law instead of in the failure criteria. Langlie and Cheng [22] also developed failure criteria based on local failure mechanisms to be used for composites subject to high strain rate impact, but utilized a maximum stress type of approach instead of a quadratic stress interaction approach for each of the failure modes. In another approach to the problem, Pecknold and Rahman [23] utilized a micromechanics model to predict the deformation response of the composite, and also utilized failure criteria based on the local stress states in each of the constituents (fiber or matrix). The prior research discussed here indicates that a failure criterion based on approximating local failure mechanisms may produce good predictions. A mechanism based failure criterion would also facilitate the development of a material degradation model when applied to the analysis of structures composed of composite materials.

## REVISED EFFECTIVE INELASTIC STRAIN CALCULATIONS

### Overview

In the composite micromechanics model [2], the composite unit cell is divided into four subcells, one fiber subcell and three matrix subcells (Figure 1). A square, periodic fiber packing is assumed. Perfect bonding between the fiber and matrix is also assumed. Appropriate uniform stress and uniform strain assumptions are then utilized to compute

the stress in each subcell based on the total strain levels and the inelastic strain in each subcell. Further details of the model can be found in [2].

In the original formulation of the model, the effective inelastic strain for the composite ply was computed by simply taking the volume weighted average of the inelastic strain in each of the subcells, as follows:

$$\varepsilon_{ij}^I = (k_f) \varepsilon_{ijAf}^I + (\sqrt{k_f})(1 - \sqrt{k_f})(\varepsilon_{ijAm}^I + \varepsilon_{ijB1}^I) + (1 - \sqrt{k_f})^2 (\varepsilon_{ijB2}^I) \quad (1)$$

where the subcells are as identified in Figure 1 and “ $k_f$ ” is the fiber volume ratio. The effective inelastic strain is required for proper application of the Poisson strains, which are utilized in the stand alone computer code within which the model is currently implemented.

By utilizing this method of computing the effective inelastic strain, however, the deformation response predicted for shear dominated fiber orientation angles differed significantly from that predicted by the Generalized Method of Cells (GMC) [24], a commonly used micromechanics analysis method. GMC, being a well developed methodology, is assumed to give “accurate” micromechanics predictions and thus provides a reasonable benchmark to compare the results predicted using the micromechanics methods developed in this study. However, the micromechanics method considered here was two to three times more computationally efficient than the version of GMC that was available at the time of this study. Furthermore, the computer code for implementing the micromechanics equations is very compact, which facilitated the implementation of the failure criteria discussed later in this report, and will most likely simplify the implementation of the micromechanics into a finite element code.

As an example, Figure 2 shows results predicted for an IM7/977-2 laminate with a  $[10^\circ]$  fiber orientation. As is seen in the figure, the results predicted using the two micromechanics methods are significantly different, which was discussed in reference [2]. At the time that reference [2] was published, a reason for the discrepancy had not been determined. As will be shown later in this report, improving the calculation of the effective inelastic strain in the micromechanics method developed for this study helped to reduce this discrepancy.

To improve the calculation of the effective inelastic strains, the fundamental assumptions and derivation techniques that were used in [2] to compute the stresses in each subcell given the total strains are applied. Appropriate uniform stress and uniform strain assumptions were applied in order to relate the macroscopic stresses to the macroscopic strains for each coordinate direction. From these expressions, the effective inelastic strains can be determined. While Poisson effects are very important in general in computing total strains, in the calculation of the effective inelastic strains Poisson effects are neglected to simplify the mathematics. The Poisson effects most likely have a minimal contribution to the effective inelastic strain. In the following derivation, Poisson effects are not included in any calculations, since only the results for the inelastic strains are utilized from this derivation. In the full micromechanics equations presented in

reference [2], Poisson effects are fully included in computing the stress levels in each subcell based on the total strain and the subcell inelastic strains. Neglecting Poisson effects in certain calculations is actually very common in mechanics of materials approaches for composite micromechanics, as is discussed in references such as [11] and [14].

Only the derivations for the normal “11” and “22” direction and in-plane shear effective inelastic strains will be shown in detail. The expression for the “33” direction inelastic strain is very similar to that of the “22” direction value and will be discussed briefly. The expressions for the out-of-plane shear follow in a similar manner to that of the in-plane shear strain. An important point to note is that while the derivations will look very similar to what was presented in [2], the derivations that follow are only meant to replace Equation (1) for the calculation of the effective inelastic strain in the composite. The remaining micromechanics calculations remain unchanged from what was presented in reference [2].

### Effective Inelastic Strain Derivation

The unit cell utilized in the development of the micromechanics equations is shown in Figure 1. The bottom layer of subcells, with subcells “Af” and “Am”, is referred to as Row 1 (R1). The top layer of subcells, with subcells “B1” and “B2”, is referred to as Row 2 (R2). Subcell “Af” is composed of fiber material, the remaining three subcells are composed of matrix material. The subscript “f” will be used to denote fiber related properties, and the subscript “m” will be used to denote matrix related properties. Subscripts “Af”, “Am”, “B1” and “B2” will be used to denote stresses and strains of the individual subcells. Subscripts “R1” and “R2” will be used to denote stresses and strains in the corresponding regions as defined above. Stresses and strains with no region identifying subscript will be assumed to represent the total effective stresses and strains for the unit cell. A superscript “I” will be used to denote inelastic strains. The subscripts “11”, “22” and “33” will be used to define normal stresses, strains, and their material properties, with the coordinate directions as defined in Figure 1. The “1” direction is along the fiber axis, directions “2” and “3” are perpendicular to the fiber axis. As is shown in Figure 1, the “2” direction is in the plane of the laminate, and the “3” direction is through the thickness of the laminate. The subscripts “12”, “13” and “23” will be used to define shear stresses, strains, and their material properties.

The symbol “E” represents the elastic modulus and the symbol “G” represents the shear modulus. The symbol “ $\sigma_{ij}$ ” represents stress tensor components, the symbol “ $\epsilon_{ij}$ ” represents strain tensor components, and the symbol “ $\gamma_{ij}$ ” represents engineering shear strain components, all assigned in a Cartesian frame of reference. The symbol “ $k_f$ ” represents the fiber volume ratio of the composite. The fibers are assumed to be transversely isotropic with properties  $E_{11f}$  representing the longitudinal elastic modulus of the fiber (along the 1 direction axis in Figure 1),  $E_{22f}$  representing the transverse modulus of the fiber, and  $G_{12f}$  representing the in-plane shear modulus of the fiber. The matrix is assumed to be an isotropic material with  $E_m$  representing the elastic modulus of the matrix and  $G_m$  representing the shear modulus of the matrix.

The stress and strain in each subcell are assumed to be the effective stress and strain, equal to the average stress or strain over the volume of the subcell. These values are assumed to be uniform over the volume of the subcell. The effective stress and strain in Row 1 and Row 2 are defined as the volume average of the stresses and strains in the corresponding subcells. The effective stress and strain in the unit cell are defined as the volume average of the stresses and strains in Row 1 and Row 2. To determine the volume average, a weighted sum is computed where the value (stress or strain) in each subcell or region is weighted by the ratio of the volume of the subcell (or region) over the total volume of the region (or unit cell).

Neglecting Poisson effects, the constitutive equations for the normal and in-plane shear stresses are given by the following expressions:

$$\sigma_{11} = E_{11}(\epsilon_{11} - \epsilon_{11}^I) \quad (2)$$

$$\sigma_{22} = E_{22}(\epsilon_{22} - \epsilon_{22}^I) \quad (3)$$

$$\sigma_{12} = G_{12}(\gamma_{12} - 2 * \epsilon_{12}^I) \quad (4)$$

The inelastic strain values are only utilized when the matrix material is considered. Since the fiber is linearly elastic, no inelastic strains are present in the fiber. For the isotropic matrix, furthermore,  $E_{11}$  is set equal to  $E_{22}$ .

### Normal Effective Inelastic Strains

In computing the normal direction (11 and 22) effective inelastic strains, the following uniform stress and uniform strain assumptions are made:

$$\begin{aligned} \epsilon_{11Af} &= \epsilon_{11Am} = \epsilon_{11R1} \\ \epsilon_{11B1} &= \epsilon_{11B2} = \epsilon_{11R2} \end{aligned} \quad (5)$$

$$\epsilon_{11R1} = \epsilon_{11R2} = \epsilon_{11}$$

$$\sigma_{22Af} = \sigma_{22Am} = \sigma_{22R1} \quad (6)$$

$$\sigma_{22B1} = \sigma_{22B2} = \sigma_{22R2}$$

$$\epsilon_{22R1} = \epsilon_{22R2} = \epsilon_{22} \quad (7)$$

The effective stresses and strains in Row 1 (R1) and Row 2 (R2), as well as for the composite unit cell, are computed using volume averaging, yielding the following expressions:

$$\epsilon_{22R1} = \sqrt{k_f} * \epsilon_{22Af} + (1 - \sqrt{k_f}) * \epsilon_{22Am} \quad (8)$$

$$\varepsilon_{22R2} = \sqrt{k_f} * \varepsilon_{22B1} + (1 - \sqrt{k_f}) * \varepsilon_{22B2} \quad (9)$$

$$\sigma_{11R1} = \sqrt{k_f} * \sigma_{11Af} + (1 - \sqrt{k_f}) * \sigma_{11Am} \quad (10)$$

$$\sigma_{11R2} = \sqrt{k_f} * \sigma_{11B1} + (1 - \sqrt{k_f}) * \sigma_{11B2} \quad (11)$$

$$\sigma_{11} = \sqrt{k_f} * \sigma_{11R1} + (1 - \sqrt{k_f}) * \sigma_{11R2} \quad (12)$$

$$\sigma_{22} = \sqrt{k_f} * \sigma_{22R1} + (1 - \sqrt{k_f}) * \sigma_{22R2} \quad (13)$$

By utilizing the constitutive equations for the fiber and matrix, along with the uniform stress and uniform strain assumptions, the following expressions are obtained for the effective inelastic normal strains:

$$\varepsilon_{11}^I = \frac{(1 - \sqrt{k_f})E_m (\sqrt{k_f} (\varepsilon_{11Am}^I + \varepsilon_{11B1}^I) + (1 - \sqrt{k_f})\varepsilon_{11B2}^I)}{(k_f)E_{11f} + (1 - k_f)E_m} \quad (14)$$

$$\varepsilon_{22}^I = \frac{(1 - \sqrt{k_f})E' \varepsilon_{22Am}^I + E_m (1 - \sqrt{k_f}) (\sqrt{k_f} \varepsilon_{22B1}^I + (1 - \sqrt{k_f}) \varepsilon_{22B2}^I)}{E' + (1 - \sqrt{k_f})E_m} \quad (15)$$

where:

$$E' = \frac{\sqrt{k_f} E_{22f} E_m}{E_m \sqrt{k_f} + E_{22f} (1 - \sqrt{k_f})} \quad (16)$$

The effective inelastic strain in the “33” direction can also be computed by using Equation (15) by switching the inelastic strains in subcells “Am” and “B1” in the expression.

### In-Plane Shear Effective Inelastic Strains

In computing the contribution from the in-plane shear (12) direction to the effective inelastic strain, the following uniform stress and uniform strain assumptions are made:

$$\gamma_{12R1} = \gamma_{12R2} = \gamma_{12} \quad (17)$$

$$\sigma_{12Af} = \sigma_{12Am} = \sigma_{12R1} \quad (18)$$

$$\sigma_{12B1} = \sigma_{12B2} = \sigma_{12R2}$$

By applying volume averaging, the effective in-plane shear stresses and strains in each region and for the composite unit cell are defined as follows:

$$\gamma_{12R1} = \sqrt{k_f} * \gamma_{12Af} + (1 - \sqrt{k_f}) * \gamma_{12Am} \quad (19)$$

$$\gamma_{12R2} = \sqrt{k_f} * \gamma_{12B1} + (1 - \sqrt{k_f}) * \gamma_{12B2}$$

$$\sigma_{12} = \sqrt{k_f} * \sigma_{12R1} + (1 - \sqrt{k_f}) * \sigma_{12R2} \quad (20)$$

By utilizing the constitutive equations for the fiber and matrix, along with the uniform stress and uniform strain assumptions, the following expression is obtained for the effective inelastic in-plane shear strain:

$$\epsilon_{12}^I = \frac{(1 - \sqrt{k_f}) G' \epsilon_{12Am}^I + G_m (1 - \sqrt{k_f}) (\sqrt{k_f} \epsilon_{12B1}^I + (1 - \sqrt{k_f}) \epsilon_{12B2}^I)}{G' + (1 - \sqrt{k_f}) G_m} \quad (21)$$

where:

$$G' = \frac{\sqrt{k_f} G_{12f} G_m}{G_m \sqrt{k_f} + G_{12f} (1 - \sqrt{k_f})} \quad (22)$$

The effective inelastic strain in the out-of-plane shear (13) direction can be computed by using Equation (21) by switching the inelastic strains in subcells “Am” and “B1” in the expression. The effective inelastic strain in the out-of-plane shear (23) direction follows automatically from the derivation presented in [2], and is presented without further comment. Note that since the fibers are assumed to be linearly elastic, this equation is identical to Equation (1) for this particular strain component.

$$\epsilon_{23}^I = (1 - \sqrt{k_f}) * (\sqrt{k_f} * (\epsilon_{23Am}^I + \epsilon_{23B1}^I) + (1 - \sqrt{k_f}) * \epsilon_{23B2}^I) \quad (23)$$

## Discussion

The revised effective inelastic strain formulations were applied to the deformation analysis of two polymer matrix composites: IM7/977-2 and AS4/PEEK (see References [1,2] for a full description of these materials and their material properties). The predicted stress-strain response for fiber orientations in which normal stresses dominate ( $[0^\circ]$ ,  $[90^\circ]$ ,  $[45^\circ]$ ) did not vary significantly from the results predicted using the original formulation. However, for fiber orientations in which shear stresses dominate ( $[10^\circ]$ ,  $[15^\circ]$ ,  $[30^\circ]$ ), the results predicted by using the revised formulation were much softer than were predicted by the original formulation. This result is demonstrated in Figure 3, which displays the stress-strain results for the IM7/977-2 laminate with a  $[10^\circ]$  fiber orientation using the revised inelastic strain formulation. By comparing the results in

Figure 2 and Figure 3, the results predicted in Figure 3 using the revised formulation almost exactly match the results predicted using GMC shown in Figure 2. These results indicate that a major contribution to the original discrepancies between the two micromechanics methods is most likely due to the method utilized to calculate the effective inelastic strain in the mechanics of materials approach. However, since the predicted deformation response is significantly softer than the experimental values, the results further suggest that the shear stresses in the polymer are not being computed accurately. The modifications to the original constitutive equations required to improve the calculation of the shear stresses in the polymer are presented in the next section of this report.

## REVISED POLYMER CONSTITUTIVE MODEL

### Original Constitutive Equations

The Ramaswamy-Stouffer viscoplastic state variable model [25], which was originally developed for metals, was utilized to simulate the rate dependent inelastic response of the polymer matrix materials in previous analyses [1,2]. As discussed in [1], there are sufficient similarities between the inelastic deformation response of metals and the inelastic response of polymers to permit the use of constitutive equations that were developed for metals to analyze polymers. The effects of hydrostatic stress on the inelastic strains were neglected in this original work. In the Ramaswamy-Stouffer equations, the inelastic strain rate,  $\dot{\epsilon}_{ij}^I$ , is defined as a function of the overstress, or difference between the deviatoric stress components,  $S_{ij}$ , and back stress state variable components,  $\Omega_{ij}$ , in the form:

$$\dot{\epsilon}_{ij}^I = D_o \exp\left[-\frac{1}{2}\left(\frac{Z_o^2}{3K_2}\right)^n\right] * \frac{S_{ij} - \Omega_{ij}}{\sqrt{K_2}} \quad (24)$$

where  $D_o$ ,  $Z_o$ , and  $n$  are material constants, and  $K_2$  is defined as follows:

$$K_2 = \frac{1}{2}(S_{ij} - \Omega_{ij})(S_{ij} - \Omega_{ij}) \quad (25)$$

The elastic components of strain are added to the inelastic strain to obtain the total strain. The following relation defines the back stress rate:

$$\dot{\Omega}_{ij} = \frac{2}{3}q\Omega_m\dot{\epsilon}_{ij} - q\Omega_{ij}\dot{\epsilon}_e^I \quad (26)$$

where  $q$  is a material constant,  $\Omega_m$  is a material constant, which represents the maximum value of the back stress, and  $\dot{\epsilon}_e^I$  is the effective inelastic strain rate, defined as follows:

$$\dot{\epsilon}_e^I = \sqrt{\frac{2}{3}\dot{\epsilon}_{ij}\dot{\epsilon}_{ij}} \quad (27)$$

where repeated indices indicate summation using the standard indicial notation definitions. Equation (26) differs slightly from the expression as given in [25] in that the original equations included a stress rate term in the evolution equation, which was not required here.

To obtain the material constants for this material model, the saturation stress values (the stress level where the stress-strain curve flattens out) from several constant strain rate tensile tests are utilized. In addition, the average inelastic strain at saturation is used. Equations (24)-(27) and linear regression techniques are then applied to obtain the material constants. More details on the constitutive equations and obtaining the material constants can be found in [1].

### Modification to Constitutive Equations

As discussed previously in this report, the original constitutive equations, as described above, do not appear to adequately model the shear response of the polymer. Furthermore, researchers such as Pecknold and Rahman [23], Chang et al. [15-17], and Tabiei et al. [21] have determined that the majority of the nonlinearity in the deformation response of polymer matrix composites is in the shear response. Therefore, proper simulation of the polymer shear response appears to be of critical importance. The necessity of modifying the Ramaswamy-Stouffer constitutive equations in order to model polymers is not unique to this work. Rocca and Sherwood [26] utilized a modified version of the evolution law (Equation (26)), wherein they included the original stress-rate term, and they also added a term including the logarithm of the effective strain rate.

For this work, a modification of the effective stress term in the flow law (Equation (25)) was carried out to improve the modeling of the shear response of the polymer. Equation (25) can be rewritten as follows:

$$K_2 = \frac{1}{2} [K_{11} + K_{22} + K_{33} + 2(K_{12} + K_{13} + K_{23})] \quad (28)$$

The normal terms (11,22,33) in this expression maintain their original definition as suggested by Equation (25) as follows:

$$K_{11} = (S_{11} - \Omega_{11})(S_{11} - \Omega_{11}) \quad (29)$$

$$K_{22} = (S_{22} - \Omega_{22})(S_{22} - \Omega_{22}) \quad (30)$$

$$K_{33} = (S_{33} - \Omega_{33})(S_{33} - \Omega_{33}) \quad (31)$$

However, the shear terms in the effective stress definition have been modified as follows:

$$K_{12} = \alpha(S_{12} - \Omega_{12})(S_{12} - \Omega_{12}) \quad (32)$$

$$K_{13} = \alpha(S_{13} - \Omega_{13})(S_{13} - \Omega_{13}) \quad (33)$$

$$K_{23} = \alpha(S_{23} - \Omega_{23})(S_{23} - \Omega_{23}) \quad (34)$$

where:

$$\alpha = \left( \frac{\sigma_m}{\sqrt{J_2}} \right)^\beta \quad (35)$$

$$\sigma_m = \frac{1}{3}(\sigma_{11} + \sigma_{22} + \sigma_{33}) \quad (36)$$

$$J_2 = \frac{1}{2}S_{ij}S_{ij} \quad (37)$$

The primary modification to these equations is the multiplication of the shear terms in the effective stress by the parameter  $\alpha$ . In this term,  $\sigma_m$  is the mean stress,  $J_2$  is the second invariant of the deviatoric stress tensor, and  $\beta$  is a rate independent material constant. While this formulation is somewhat phenomenological in nature, relating the shear contributions to the inelastic response to the mean stress is based on actual observed physical mechanisms, as discussed earlier in this report. When the parameter  $\beta$  is set equal to zero (0), the value of  $\alpha$  in Equation (35) is equal to one (1), and Equation (28) is equivalent to Equation (25). Therefore, the modification to the constitutive equations is implemented through the use of the correlation coefficient  $\alpha$ .

Since only uniaxial tensile data was available for the polymers considered in this study, the value of the parameter  $\beta$  was determined empirically by fitting composite data with shear dominated fiber orientation angles, such as [10°] or [15°]. Analyses of [45°] laminates, in which the normal and shear stresses are more equivalent on the material axis level, were then conducted in order to verify that the determined constant value was reasonable. Ideally, the polymer model would be characterized by using a combination of tension, torsion, and tension-torsion tests done on the bulk polymer. Since composite data was utilized to characterize the model, simplified, consistent techniques to characterize the polymer using bulk polymer data have not yet been determined. The remaining material constants were determined using techniques described in [1].

### Material Properties for Verification Analyses

To verify the micromechanics equations, a series of analyses were carried out using two material systems. For consistency, the same two materials systems examined in [2] were utilized. Both material systems exhibit a nonlinear deformation response for off-axis fiber orientation angles. The first material system, supplied by Fiberite, Inc., consists of carbon IM-7 fibers in a 977-2 toughened epoxy matrix. Unidirectional laminates with fiber orientations of [0°], [10°], [45°], and [90°] were tested. Tensile tests were conducted by Cincinnati Testing Labs of Cincinnati, Ohio at a strain rate of

1E-04 /sec on each of the composites [27]. As discussed in [1,2], only low strain rate data were obtained at this time.

The IM7/977-2 composite has a fiber volume ratio of 0.60. The material properties of the IM-7 fibers, as determined from Reference [28], are stated in Table 1. The elastic properties of the Fiberite 977-2 toughened epoxy, as determined in Reference [1], are stated in Table 2. The inelastic properties for the Fiberite 977-2 matrix for low strain rate tensile loading, required for the modified Ramaswamy-Stouffer constitutive equations, are stated in Table 2. All the constants were determined in [1], with the exception of  $\beta$ , which is new. The value for “q” was varied somewhat from that utilized in [1] in order to provide a slightly better fit to the composite data. Since approximations were required to determine the inelastic material constants for this material originally [1], making slight adjustments to the constants was considered to be acceptable.

The second material that was studied consists of carbon AS4 fibers in a PEEK thermoplastic matrix. Tensile stress-strain curves were obtained by Weeks and Sun [29] for unidirectional composites with fiber orientations of [14°], [30°], [45°] and [90°] at a strain rate of 1E-05 /sec, and composites with fiber orientations of [15°], [30°], [45°] and [90°] at a strain rate of 0.1 /sec.

The fiber volume ratio used for the AS4/PEEK material was 0.62 (a typical value for this material based on representative manufacturer information). The elastic properties of the AS-4 fibers, as listed in Reference [30], are shown in Table 1. For the PEEK matrix, the elastic properties are shown in Table 2 [1]. The inelastic material constants for the modified Ramaswamy-Stouffer constitutive equations were determined in [1] (except again for  $\beta$ , which is new) and are shown in Table 2.

	Longitudinal Modulus (GPa)	Transverse Modulus (GPa)	Poisson’s Ratio	In-Plane Shear Modulus (GPa)
IM-7	276	13.8	0.25	20.0
PEEK	214	14.0	0.20	14.0

**Table 1: Elastic Properties for Fibers Used in Composite Laminates**

	E (GPa)	$\nu$	$D_o$ (1/sec)	N	$Z_o$ (MPa)	q	$\Omega_m$ (MPa)	$\beta$
977-2	3.65	0.40	1E+04	0.50	1030	100	69	1.2
PEEK	4.00	0.40	1E+04	0.46	630	310	52	0.45

**Table 2: Material Properties for Polymer Matrices Used in Composite Laminates**

In Table 2, “E” represents the elastic modulus, “ $\nu$ ” is the Poisson’s ratio, and the inelastic material constants are as described earlier. There is currently no good explanation for the physical meaning of the parameter  $\beta$ . As a result, the significance of the value of the parameter and its variation for the two materials examined in this study can not be quantified at this time.

## Verification Analysis Results

Analyses were conducted using the revised polymer constitutive model implemented within the composite micromechanics model developed in [2]. The revised methodology for calculating the effective inelastic strain detailed earlier in the report was utilized for these analyses. The predicted results were compared to experimentally obtained values. Stress-strain curves for the IM7/977-2 laminates are shown in Figures 4-7. Stress-strain curves for the AS4/PEEK composite are shown in Figures 8-11 for a strain rate of 1E-05 /sec, and in Figures 12-15 for a strain rate of 0.1 /sec. The plots of the [10°] IM7/977-2 laminate shown in Figure 5, and the [14°] and [15°] AS4/PEEK laminates shown in Figures 8 and 12 are correlations, while the remaining plots are “true” predictions.

As can be seen in the figures, for both materials, and for both strain rates for the AS4/PEEK system, the analytical results match the experimental values quite well for all fiber orientation angles examined. The only major discrepancy between the experimental and computed results is that for the shear dominated fiber orientation angles ([10°], [14°], and [15°]), the inelastic portion of the predicted stress-strain curves are flatter than the experimental results. However, the predicted stresses at the end of the stress-strain curves match the experimental values reasonably well. For predicting ply strength, which will be discussed in the next section of this report, correctly predicting the stress levels at the end of the stress-strain curve is most critical. The overall comparison between the experimental and predicted values is still quite good.

The effects of modifying the polymer constitutive equation can be seen quite clearly in Figure 16, where the predicted stress-strain curves for the IM7/977-2 laminate with a [10°] degree fiber orientation angle from Figures 3 and 5 are superimposed. As can be seen from Figure 16, modifying the polymer constitutive model produced a significant improvement in predicting the deformation response for this shear dominated fiber orientation angle. The original constitutive model predicted results that were much softer than the experimental values, while the revised equations produced composite predictions that compare much more favorably to the experimental results.

## PLY STRENGTH MODEL

### Overview

In order to develop structural level penetration and failure models that can be applied to high strain rate impact applications, ply level failure needs to be accurately predicted. As discussed in the background section of this report, previous researchers have developed a variety of ply level failure models. For this work, ply level failure due to local failure mechanisms is predicted based on macroscopic stresses and strengths. In particular, the Hashin failure model [3] is utilized in this work. As discussed earlier, some researchers such as Pecknold and Rahman [23] have utilized constituent level stresses to predict ply failure based on local failure mechanisms. However, for the model presented in this work, there was a higher level of confidence in the effective stresses predicted on the macroscopic level than in the constituent level stresses predicted for each of the subcells. Furthermore,

appropriate strength data were more readily available for the composites analyzed for this study than for the individual constituents. However, particularly in considering the ultimate future application of the ply strength models, the ability to account for and predict local failure mechanisms at least approximately was desired.

Since only ply level failure based on simple tensile tests is being considered at this time, property degradation models are not being utilized. For structural level modeling, the ability to only degrade certain material properties based on the local ply failure mechanisms might be desirable to provide improved simulation of stress transfer mechanisms. Furthermore, in implementing the model into a finite element code, a gradual degradation of the material properties might improve the stability of the finite element analysis. Since the failure model utilized in this study does predict failure based on approximations of local failure mechanisms, the eventual incorporation of property degradation models will be possible.

### Hashin Failure Criterion

For this work, the Hashin failure criterion was chosen [3]. This criterion predicts ply level failure based on local failure mechanisms using macroscopic stresses and strengths. The criterion is based on stresses and strengths in the local material axis system, so appropriate transformations [25] must be carried out to convert stresses from the structural axis system to the material axis system. Since the composites analyzed in this study were only subject to in plane loading and the out-of-plane stresses were found to be relatively small, the plane stress approximation to the Hashin model was utilized. However, for applications where the out-of-plane stresses are significant, there are full three-dimensional versions of the criterion available [3].

The Hashin criterion is based on quadratic combinations of stresses and strengths. A quadratic model was chosen in order to provide the best approximation to the failure surface while still allowing for a relatively simple model [3]. Ply failure based on fiber tensile failure, fiber compressive failure, matrix tensile failure and matrix compressive failure is predicted separately. In each of the separate criteria, failure is considered to have occurred if the value of the expression is greater than one (1). For the purposes of this study, once failure in any of the failure modes is detected, total composite failure is considered to have occurred. In actuality, particularly for matrix dominated failure modes, the composite can withstand load after the “failure” load has occurred. However, for the laminate configurations examined here, final composite failure was assumed to occur shortly after initial matrix cracking takes place, therefore only the initial failure load was predicted.

Failure criteria for each of the failure modes are as follows. In each of the expressions,  $\sigma_{ij}$  is the stress component,  $X_T$  is the ply tensile strength in the longitudinal (fiber) direction, and  $X_C$  is the compressive strength in the longitudinal direction. Furthermore,  $Y_T$  is the tensile strength in the transverse direction,  $Y_C$  is the compressive

strength in the transverse direction, and S is the ply shear strength. Failure is considered to occur when the value of the expression becomes greater than or equal to one (1). Tensile fiber failure is predicted by using the following expression:

$$\left(\frac{\sigma_{11}}{X_T}\right)^2 + \left(\frac{\sigma_{12}}{S}\right)^2 = 1 \quad (38)$$

Compressive fiber failure is predicted using the following equation. Shear stresses were not included in the failure criterion since Hashin was unsure whether shear stresses increased or decreased the compressive strength. Therefore, the effects of shear stresses were neglected [3].

$$\frac{|\sigma_{11}|}{X_C} = 1 \quad (39)$$

Tensile matrix failure is predicted using the following expression:

$$\left(\frac{\sigma_{22}}{Y_T}\right)^2 + \left(\frac{\sigma_{12}}{S}\right)^2 = 1 \quad (40)$$

Compressive matrix failure is predicted by the following:

$$\left(\frac{\sigma_{22}}{2S}\right)^2 + \left[\left(\frac{Y_C}{2S}\right)^2 - 1\right] \frac{\sigma_{22}}{Y_C} + \left(\frac{\sigma_{12}}{S}\right)^2 = 1 \quad (41)$$

#### Verification Analyses: IM7/977-2 Laminates

To verify the ply strength model, the IM7/977-2 material was once again analyzed. For the IM7/977-2 system, the longitudinal tensile strength is 2300 MPa [27], the longitudinal compressive strength is 900 MPa [31], the transverse tensile strength is 73 MPa [27] and the shear strength is 85 MPa [27]. Due to a lack of data, the transverse compressive strength was set to twice the transverse tensile strength. To compute the in-plane shear strength, the failure stress of a  $[\pm 45^\circ]_s$  laminate was divided by two (2), which is a standard procedure for determining shear strength [32]. The predicted and experimental [27] failure strength values for  $[10^\circ]$  and  $[45^\circ]$  laminates for the IM7/977-2 material system are shown in Table 3. For both laminates considered, failure was predicted to be due to tensile matrix failure. The “failure stress” stated in Table 3 and all remaining tables is the longitudinal stress (stress along the loading direction) at which failure was predicted to occur. However, the values of all of the stress components at each time step were used in applying the Hashin failure criteria.

	Predicted Failure Stress (MPa)	Experimental Failure Stress (MPa)
[10°] Laminate	480	500
[45°] Laminate	100	105

**Table 3: Failure Stress Predictions for IM7/977-2 Laminate**

As can be seen in Table 3, for a shear dominated fiber orientation ([10°] laminate), and a fiber orientation with significant normal and shear stresses ([45°] laminate), the predicted failure stresses compare reasonably well to the experimental values. These results indicate that the presented failure criteria produce accurate results for a variety of fiber orientations.

Verification Analyses: AS4/PEEK Laminates

The AS4/PEEK material system considered earlier was once again analyzed. For this material, only quasi-static strength data were available. Furthermore, ply shear strength data that provided an acceptable correlation with the available experimental results were not available. In addition, transverse stresses predicted using the deformation model for off-axis composite layers (such as [30°] and [45°] laminates) were greater than the transverse strengths indicated by the Weeks and Sun data shown in Figures 10 and 14 [29]. Therefore, these values were not used for the transverse strengths. Figures 10 and 14 indicate that the transverse modulus does not appear to vary with strain rate for this material, indicating that the transverse strengths may also be rate independent. For a carbon fiber reinforced polymer matrix composite, longitudinal strengths have been found to be rate independent [33]. Therefore, for this study, the longitudinal and transverse strengths for the AS4/PEEK system were assumed to be rate independent, and the shear strength was assumed to be rate dependent.

For the AS4/PEEK material, a longitudinal tensile strength of 2070 MPa was used [34], and the transverse tensile strength was set to 83 MPa [34]. The longitudinal compressive strength was set equal to one-half of the longitudinal tensile strength, and the transverse compressive strength was set equal to twice the transverse tensile strength for this study. The shear strength values were determined by using the data from the [15°] laminates. From this data, the shear strength for a strain rate of 1E-05 /sec was determined to be 63 MPa, and the shear strength for a strain rate of 0.1 /sec was determined to be 88 MPa. Using these values, failure stresses were predicted for the [30°] and [45°] laminates for both strain rates. The predicted and experimental results for a strain rate of 1E-05 /sec are shown in Table 4, and the results for a strain rate of 0.1 /sec are shown in Table 5. In all cases, failure was predicted to be due to tensile matrix failure.

	Predicted Failure Stress (MPa)	Experimental Failure Stress (MPa)
[30°] Laminate	130	140
[45°] Laminate	98	104

**Table 4: Failure Stress Predictions for AS4/PEEK: Strain Rate=1E-05 /sec**

	Predicted Failure Stress (MPa)	Experimental Failure Stress (MPa)
[30°] Laminate	165	170
[45°] Laminate	114	112

**Table 5: Failure Stress Predictions for AS4/PEEK: Strain Rate=0.1 /sec**

For both strain rates and both fiber orientations considered, the comparison between the predicted and experimental values is quite good. The results indicate that the failure criteria are able to predict ply failure for a variety of fiber orientations and strain rates. The results for this material also indicate that even when some approximations are required in determining the ply failure stresses, reasonable results can still be obtained.

## CONCLUSIONS

In this paper, several modifications to a previously developed analytical methodology for predicting the nonlinear rate-dependent response of polymer matrix composites have been described. The constitutive equations utilized to model the inelastic, nonlinear deformation response of the polymer were modified to improve the shear response of the polymer. This improvement resulted by having the shear portion of the effective stress be dependent on the hydrostatic stress state. The composite micromechanics methodology was modified to allow for an improved calculation of the effective inelastic strain. Properly calculating the effective inelastic strain is important for the application of total Poisson strains in a strain controlled loading algorithm. Even though Poisson strains were neglected in computing the effective inelastic strains, the total Poisson strains were apparently computed accurately. Finally, the Hashin failure criterion was incorporated into the material model to allow for the calculation of ply ultimate strengths based on approximating local failure mechanisms.

For all of the modifications described in this report, verification studies were carried out using two representative carbon fiber reinforced polymer matrix composites. For both material systems studied, the deformation response and ply ultimate strengths predicted by the analytical model compared well to experimentally obtained results for a variety of ply orientations and strain rates. The results indicate that the analytical model is successful in predicting the rate-dependent, nonlinear response of polymer matrix composites.

Future work will involve developing a laminate theory to allow for the analysis of simple angle ply, symmetric laminates. The combined deformation and failure model will then be implemented into a transient dynamic finite element code. Full deformation and failure analyses will then be conducted for a high strain rate impact problem such as simulating a split Hopkinson bar experiment on a composite specimen. Ultimately, the developed methodology will be used to simulate the response of composite structures subject to a high strain rate impact.

## REFERENCES

1. Goldberg, R.K.; and Stouffer, D.C.: High Strain Rate Deformation Modeling of a Polymer Matrix Composite: Part I-Matrix Constitutive Equations. NASA TM-206969, 1998.
2. Goldberg, R.K.; and Stouffer, D.C.: High Strain Rate Deformation Modeling of a Polymer Matrix Composite: Part II-Composite Micromechanical Model. NASA TM-208664, 1998.
3. Hashin, Z.: Failure Criteria for Unidirectional Fiber Composites. *Journal of Applied Mechanics*, Vol. 47, pp. 329-334, 1980.
4. Ward, I.M.: Mechanical Properties of Solid Polymers. John Wiley and Sons, New York, 1983.
5. Ward, I.M.; and Hadley, D.W.: An Introduction to the Mechanical Properties of Solid Polymers. John Wiley and Sons, New York, 1993.
6. Ward, I.M.: Review: The Yield Behavior of Polymers. *Journal of Materials Science*, Vol. 6, pp. 1397-1417, 1971.
7. Miller, E.: Introduction to Plastics and Composites. Marcel Drekker, Inc., New York, 1996.
8. Bordonaro, C.M.: Rate Dependent Mechanical Behavior of High Strength Plastics: Experiment and Modeling. PhD Dissertation, Rensselaer Polytechnic Institute, Troy, New York, 1995.
9. Nahas, M.N.: Survey of Failure and Post-Failure Theories of Laminated Fiber-Reinforced Composites. *Journal of Composite Technology and Research*, Vol. 8, pp. 138-153, 1986.
10. Gibson, R.F.: Principles of Composite Material Mechanics., Mc-Graw Hill, New York, 1994.
11. Herakovich, C.T.: Mechanics of Fibrous Composites. John Wiley and Sons, New York, 1998.

12. Reddy, J.N.; and Pandey, A.K.: A First-Ply Failure Analysis of Composite Laminates. *Computers and Structures*, Vol. 25, pp. 371-393, 1987.
13. Sun, C.T.; and Quinn, B.J.: Evaluation of Failure Criteria Using Off-Axis Laminate Specimens. Proceedings of the American Society for Composites Ninth Technical Conference, T.-W. Chou and J.R. Vinson, eds., Technomic Publishing Co., Lancaster, PA., 1994.
14. Agarwal, B.D.; and Broutman, L.J.: Analysis and Performance of Fiber Composites. John Wiley and Sons, New York, 1990.
15. Chang, F.-K.; Scott, R.A.; and Springer, G.S.: Failure Strength of Nonlinearly Elastic Composite Laminates Containing a Pin Loaded Hole. *Journal of Composite Materials*, Vol. 18, pp. 464-477, 1984.
16. Chang, F.-K.; and Chang, K.-Y.: Post-Failure Analysis of Bolted Composite Joints in Tension or Shear-Out Mode Failure. *Journal of Composite Materials*, Vol. 21, pp. 809-833, 1987.
17. Chang, F.K.; and Chang, K.-Y.: A Progressive Damage Model for Laminated Composites Containing Stress Concentrations. *Journal of Composite Materials*, Vol. 21, pp. 834-855, 1987.
18. Yen, C.-F.: Analysis of Impact Damage Progression in Composite Structures. Proceedings of the 5<sup>th</sup> International LS-DYNA Users Conference, Southfield, MI, 1998.
19. Banerjee, R.: Numerical Simulation of Impact Damage in Composite Laminates. Proceedings of the American Society for Composites Seventh Technical Conference, H.T. Hahn, ed., Technomic Publishing Co., Lancaster, PA., 1992.
20. Rotem, A.: Prediction of Laminate Failure with the Rotem Failure Criterion. *Composites Science and Technology*, Vol. 58, pp. 1083-1094, 1998.
21. Tabiei, A.; Yiang, Y.; and Simitzes, G.J.: Compressive Behavior of Moderately Thick Plates with Progressive Damage. *Mechanics of Composite Materials and Structures*, Vol. 4, pp. 281-295, 1997.
22. Langlie, S.; and Cheng, W.: Numerical Simulation of High Velocity Impact on Fiber-Reinforced Composites,. *ASME Pressure Vessels and Piping Division (Publication) PVP.*, ASME, Vol. 159, pp. 51-64, 1989.
23. Pecknold, D.A.; and Rahman, S.: Application of a New Micromechanics-Based Homogenization Technique for Nonlinear Compression of Thick-Section Laminates. Compression Response of Composite Structures, ASTM STP 1185, S.E. Groves and A.L. Highsmith, eds., American Society for Testing and Materials, pp. 34-54, 1994.

24. Wilt, T.E.; and Arnold, S.M.: Micromechanics Analysis Code (MAC) User Guide: Version 2.0. NASA TM-107290, National Aeronautics and Space Administration, 1996.
25. Stouffer, D.C.; and Dame, L.T.: Inelastic Deformation of Metals. Models, Mechanical Properties and Metallurgy. John Wiley and Sons, New York, 1996.
26. Rocca, D.P.; and Sherwood, J.A.: Impact of Steel Projectiles into Thin Polycarbonate Lenses using a Unified State Variable Constitutive Model with Failure in LS-DYNA. Proceedings of the 5<sup>th</sup> International LS-DYNA Users Conference, Southfield, MI, 1998.
27. Gieseke, B.: Private Communication, Cincinnati Testing Laboratories, Inc., 1997.
28. Gates, T.S.; Chen, J.-L.; and Sun, C.T.: Micromechanical Characterization of Nonlinear Behavior of Advanced Polymer Matrix Composites. Composite Materials: Testing and Design (Twelfth Volume), ASTM STP 1274, R.B. Deo and C.R. Saff, eds., American Society of Testing and Materials, pp. 295-319, 1996.
29. Weeks, C.A.; and Sun, C.T.: Nonlinear Rate Dependence of Thick-Section Composite Laminates. High Strain Rate Effects on Polymer, Metal and Ceramic Matrix Composites and Other Advanced Materials, AD-Vol. 48, Y.D.S. Rajapakse and J.R. Vinson, eds., ASME, pp. 81-95, 1995.
30. Murthy, P.L.N.; Ginty, C.A.; and Sanfeliz, J.G.: Second Generation Integrated Composite Analyzer (ICAN) Computer Code. NASA TP-3290, National Aeronautics and Space Administration, 1993.
31. Smith, D.L.; and Dow, M.B.: Properties of Three Graphite/Toughened Epoxy Resin Composites. NASA TP-3102, 1991.
32. Daniel, I.M.; and Ishai, O.: Engineering Mechanics of Composite Materials. Oxford University Press, New York, 1994.
33. Daniel, I.M.; Hamilton, W.G.; and LaBedz, R.H.: Strain Rate Characterization of Unidirectional Graphite/Epoxy Composite. Composite Materials: Testing and Design (Sixth Conference), ASTM STP 787, I.M. Daniel, ed., American Society for Testing and Materials, pp. 393-413, 1982.
34. Coquill, S.L.; and Adams, D.F.: Mechanical Properties of Several Neat Polymer Matrix Materials and Unidirectional Carbon Fiber-Reinforced Composites. NASA CR-18105, 1989.

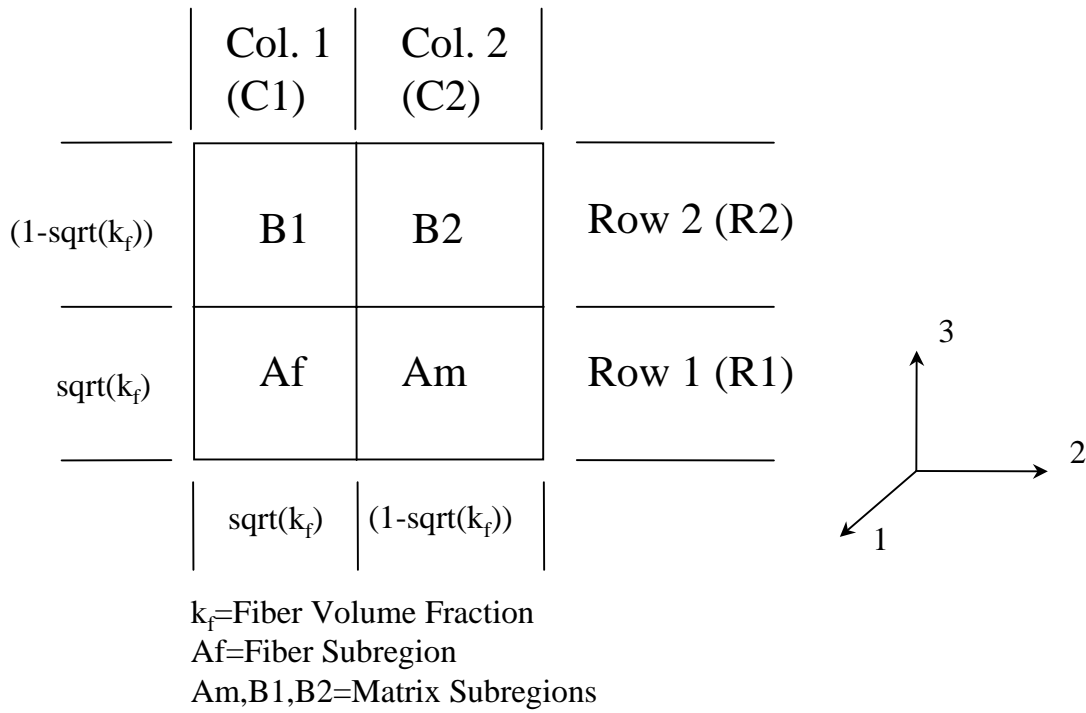


**Figure 1: Geometry and Layout of Mechanics of Materials Unit Cell Model.**

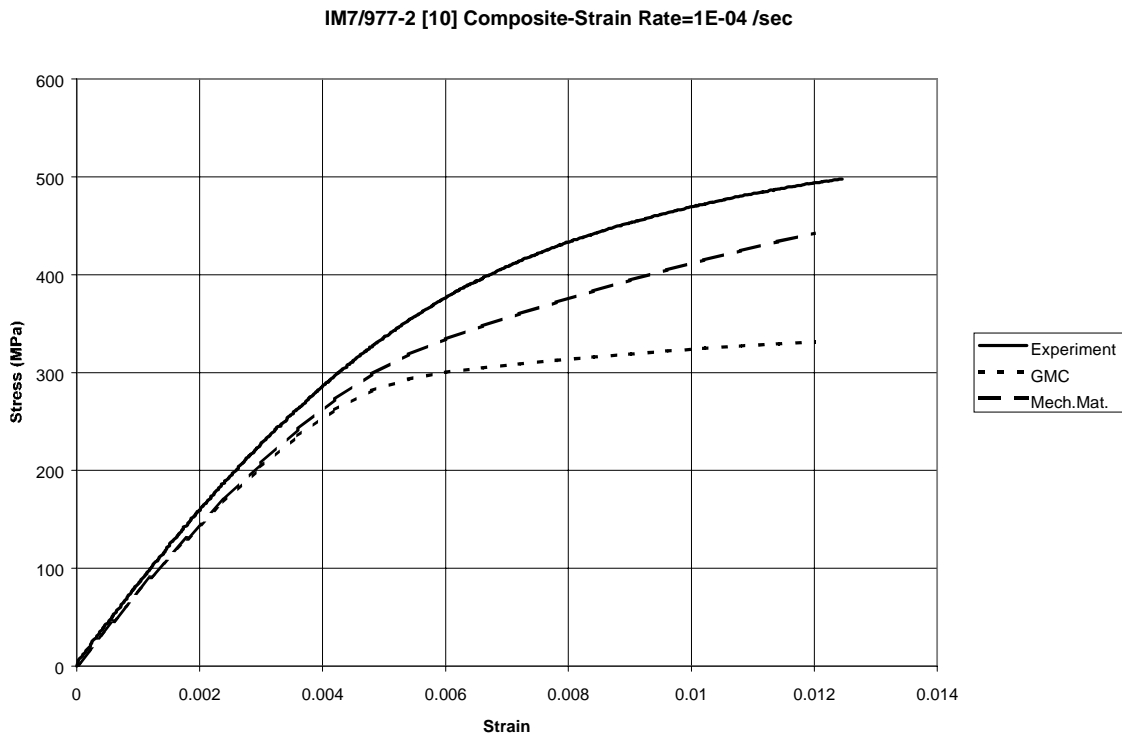


**Figure 2: Model Predictions for IM7/977-2 [10°] Laminate Using Original Inelastic Strain Formulation for Mechanics of Materials Approach**

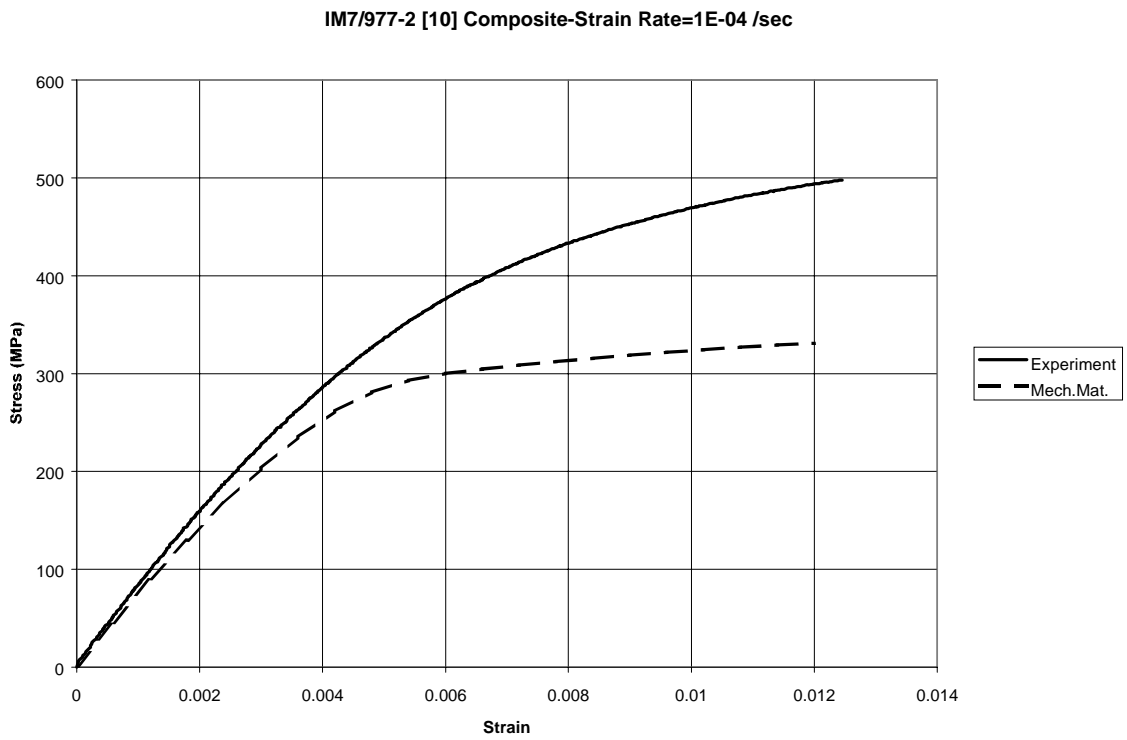


**Figure 3: Model Predictions for [10°] IM7/977-2 Laminate with Revised Inelastic Strain Calculations**

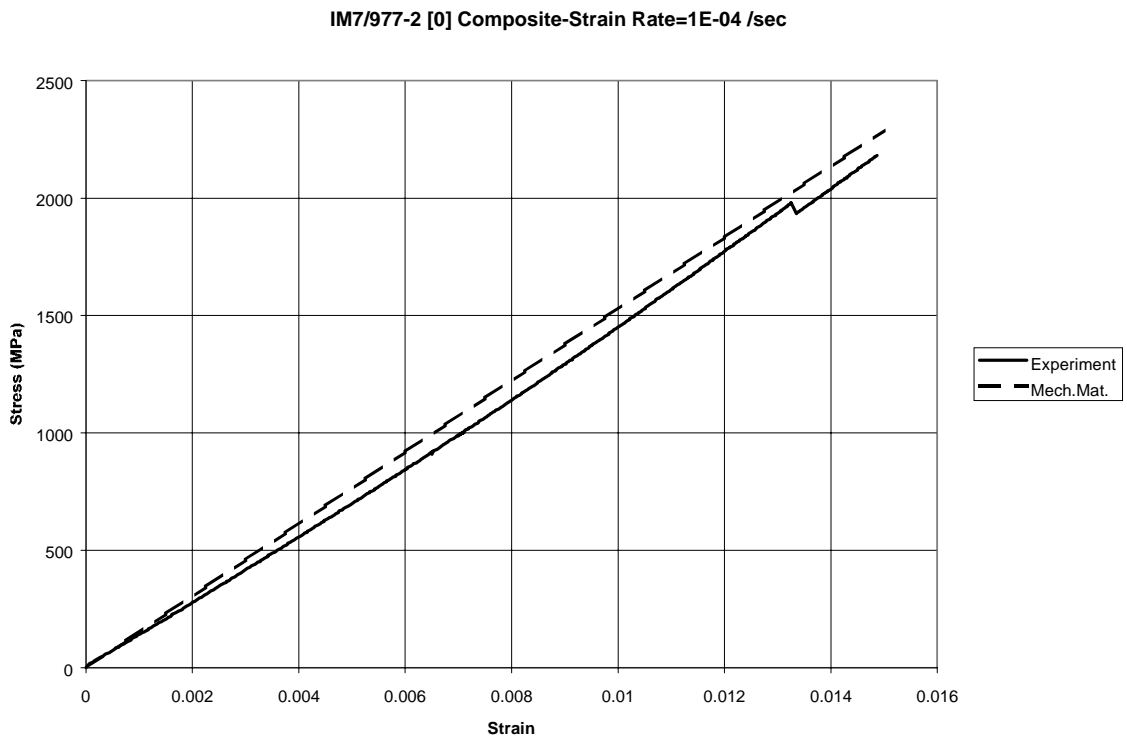


**Figure 4: Model Predictions for [0°] IM7/977-2 Laminate with Revised Polymer Model**

IM7/977-2 [10] Composite-Strain Rate=1E-04 /sec

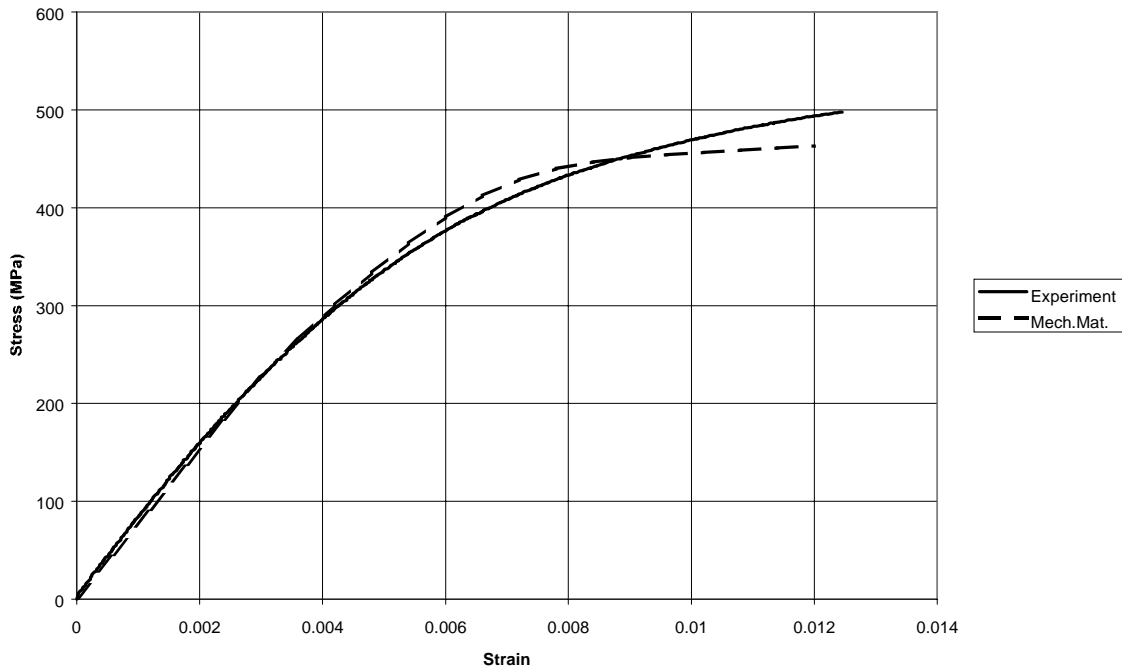


Figure 5: Model Predictions for [10°] IM7/977-2 Laminate with Revised Polymer Model

IM7/977-2 [45] Composite-Strain Rate=1E-04 /sec

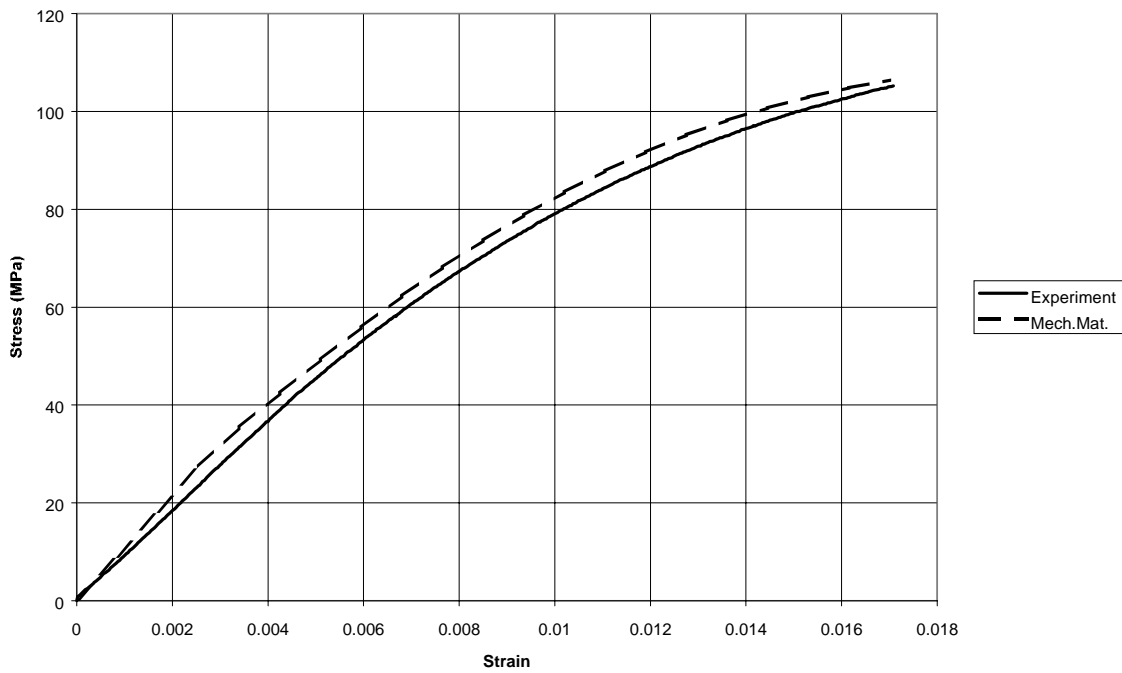


Figure 6: Model Predictions for [45°] IM7/977-2 Laminate with Revised Polymer Model

IM7/977-2 [90°] Composite-Strain Rate=1E-04 /sec

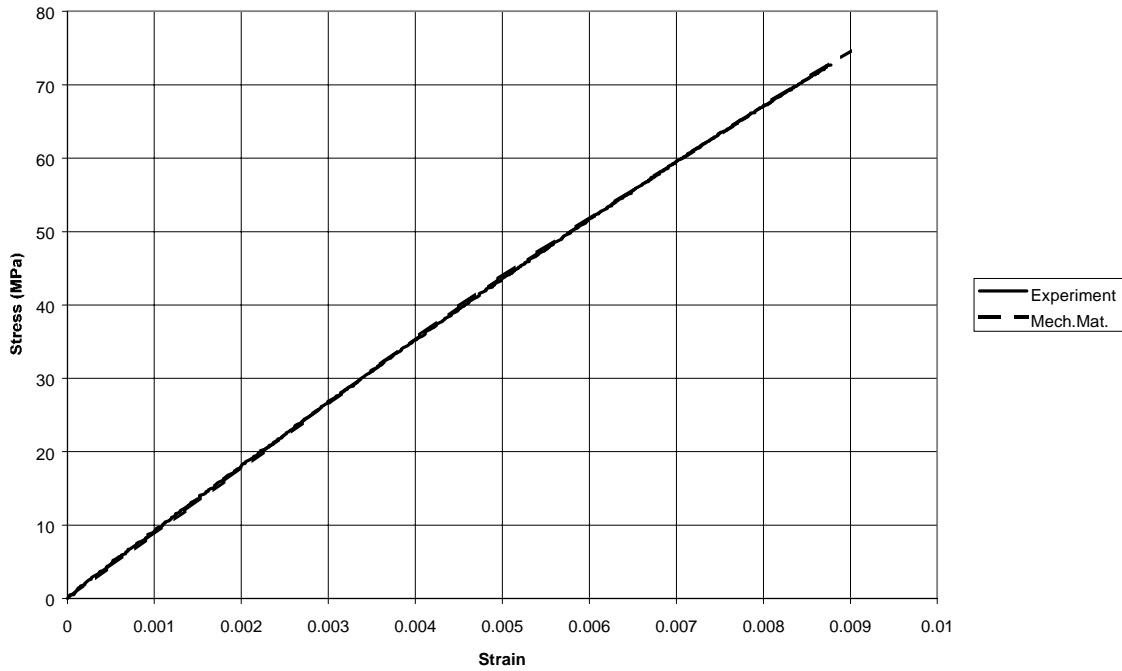


Figure 7: Model Predictions for [90°] IM7/977-2 Laminate with Revised Polymer Model

AS4/PEEK [14°] Composite-Strain Rate=1E-05 /sec

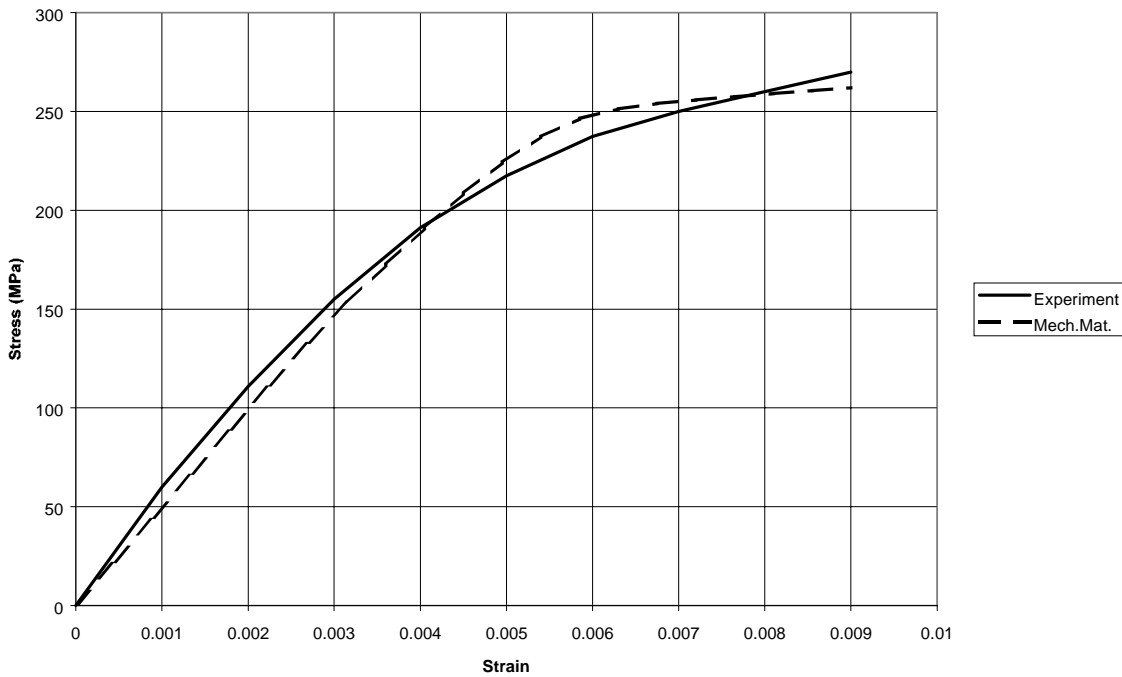


Figure 8: Model Predictions for [14°] AS4/PEEK Laminate with Revised Polymer Model-Strain Rate=1E-05 /sec

AS4/PEEK [30°] Composite-Strain Rate=1E-05 /sec

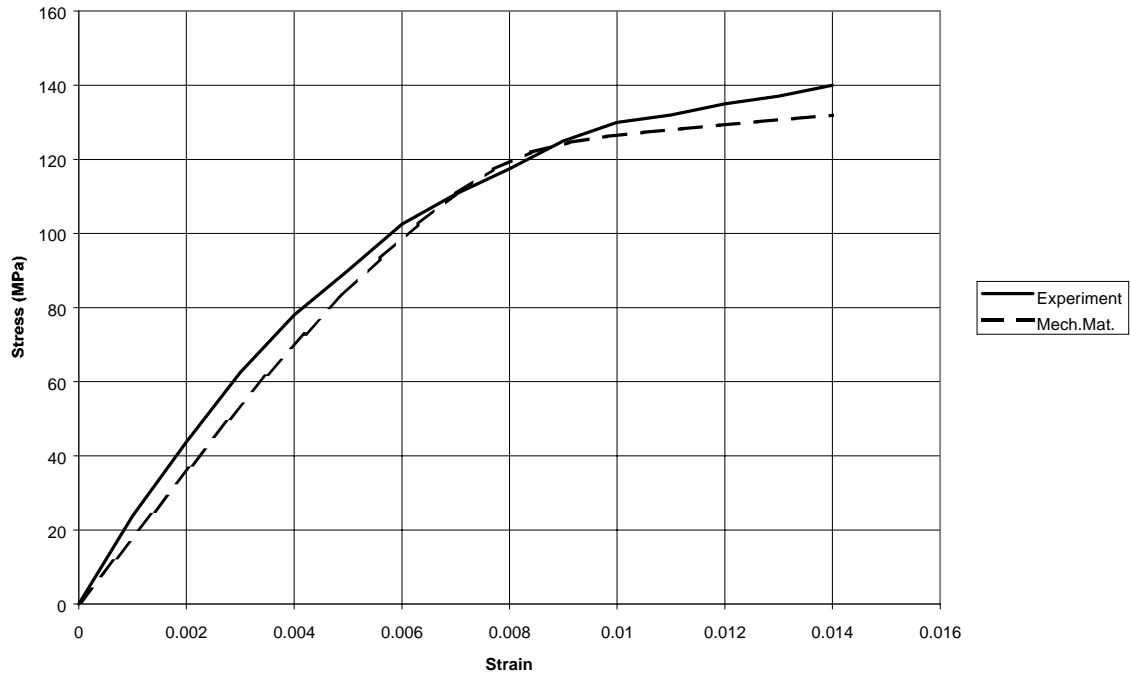


Figure 9: Model Predictions for [30°] AS4/PEEK Laminate with Revised Polymer Model-Strain Rate=1E-05 /sec

AS4/PEEK [45°] Composite-Strain Rate=1E-05 /sec

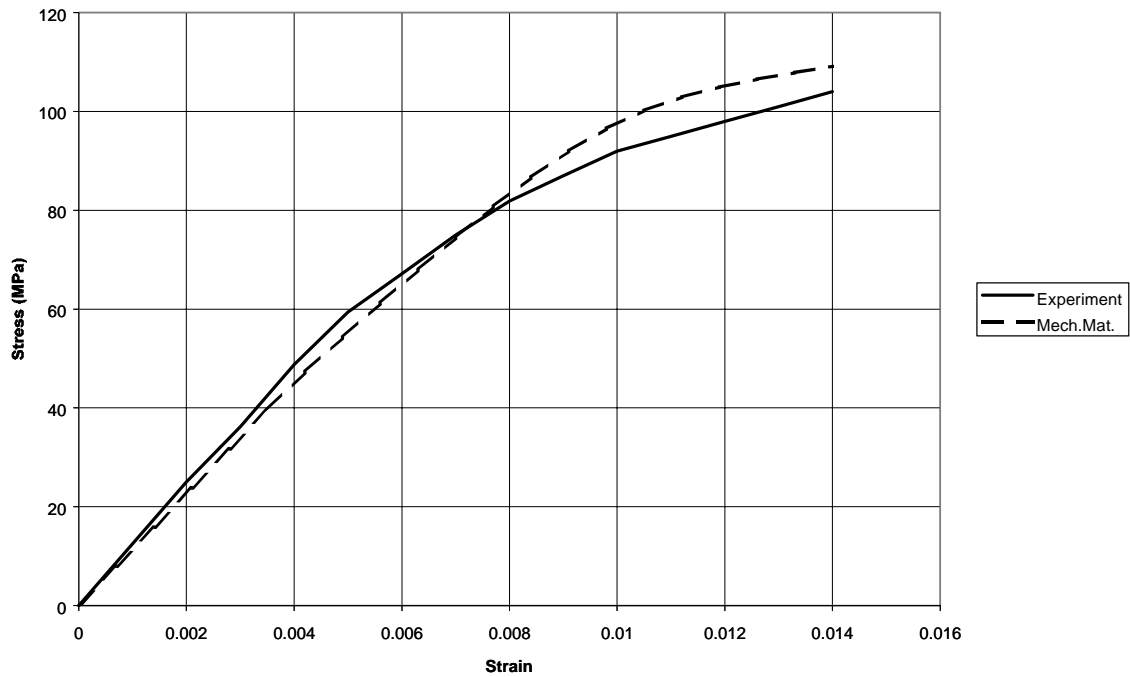
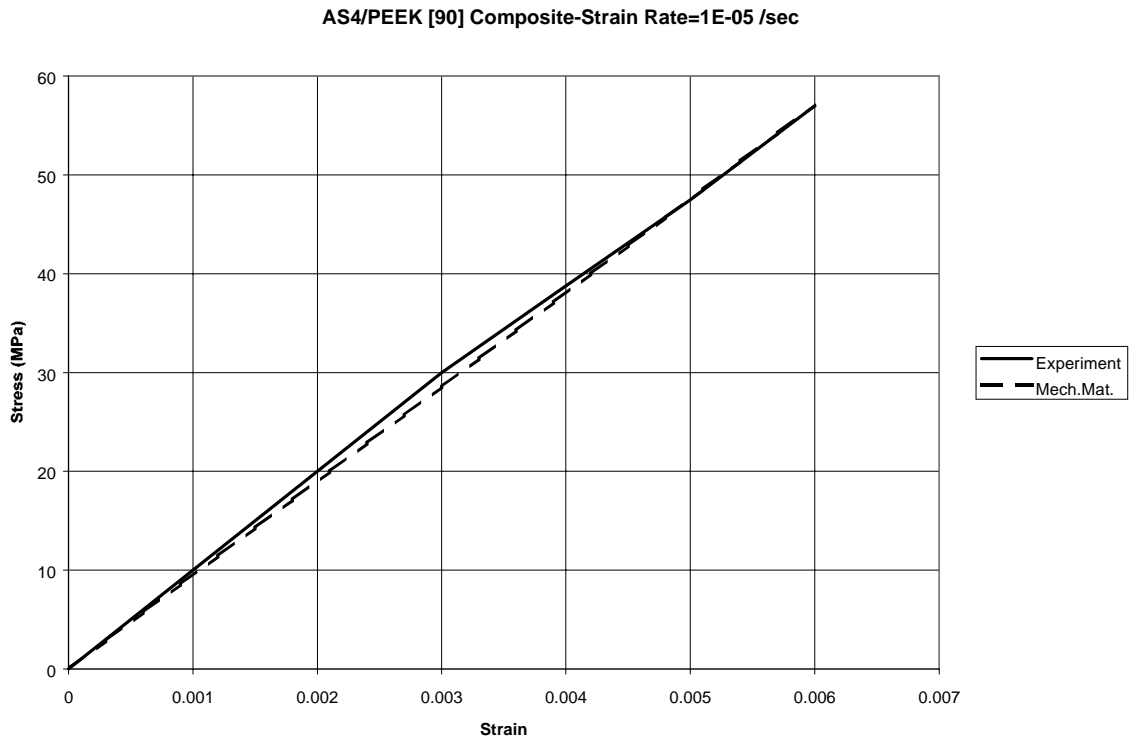
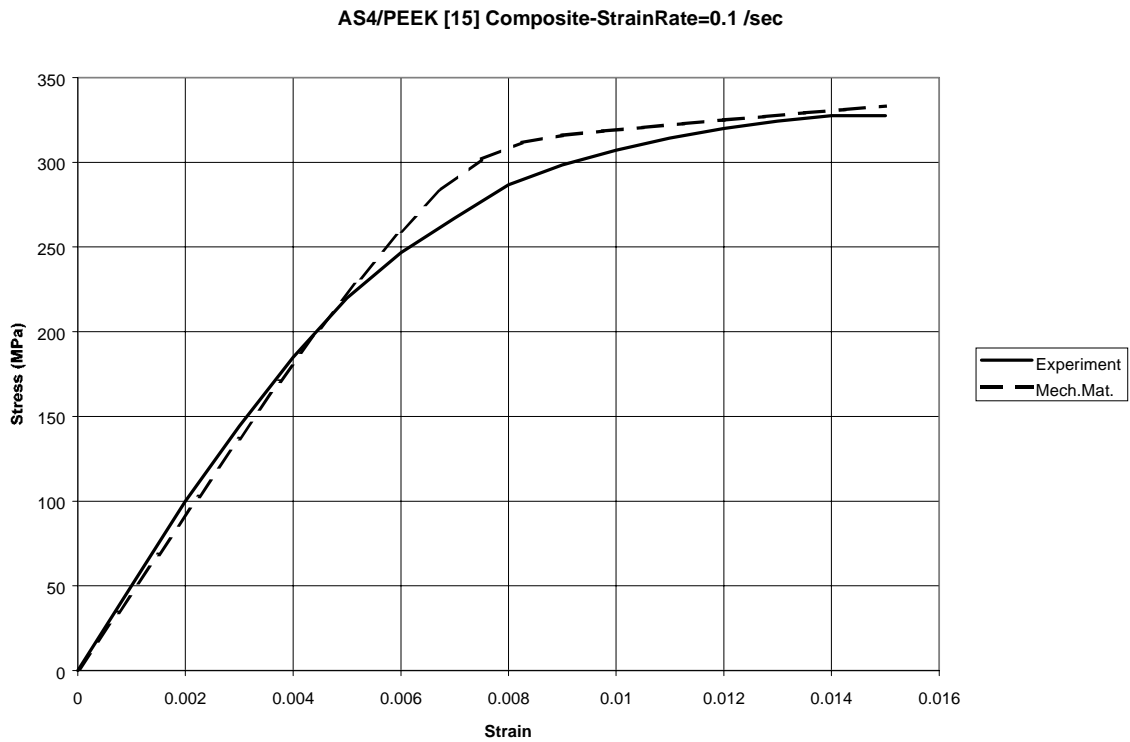


Figure 10: Model Predictions for [45°] AS4/PEEK Laminate with Revised Polymer Model-Strain Rate=1E-05 /sec



**Figure 11: Model Predictions for [90°] AS4/PEEK Laminate with Revised Polymer Model-Strain Rate=1E-05/sec**



**Figure 12: Model Predictions for AS4/PEEK [15°] Laminate with Revised Polymer Model-Strain Rate=0.1 /sec**

AS4/PEEK [30] Composite-Strain Rate=0.1 /sec

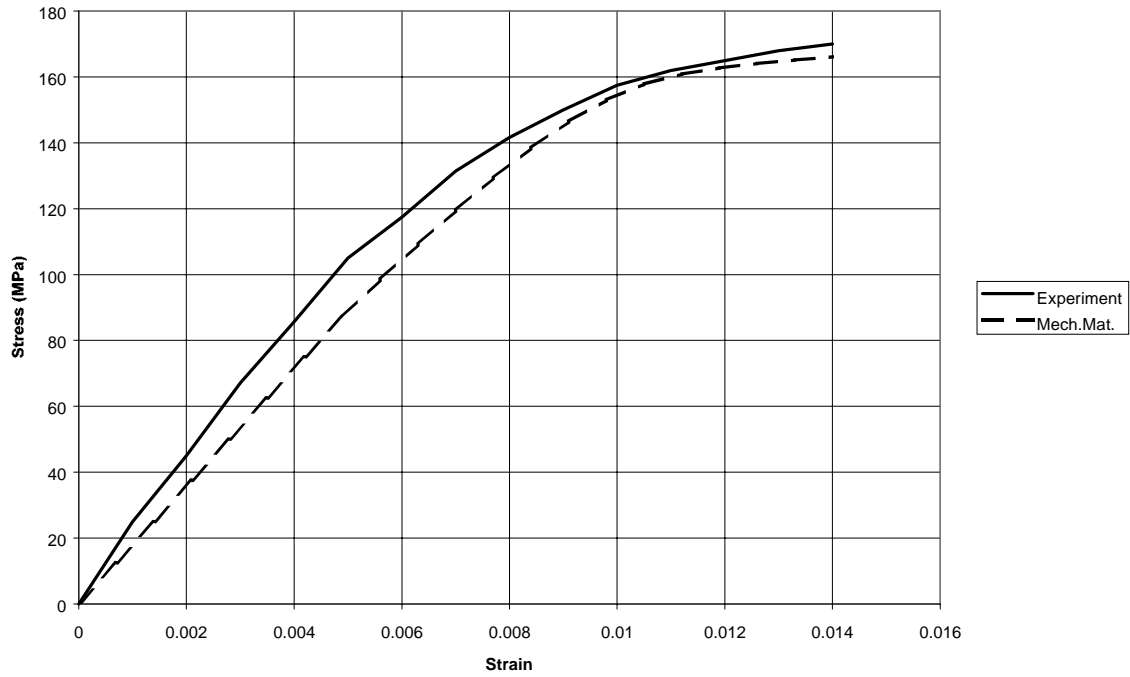


Figure 13: Model Predictions for [30°] AS4/PEEK Laminate with Revised Polymer Model-Strain Rate=0.1 /sec

AS4/PEEK [45] Composite-Strain Rate=0.1 /sec

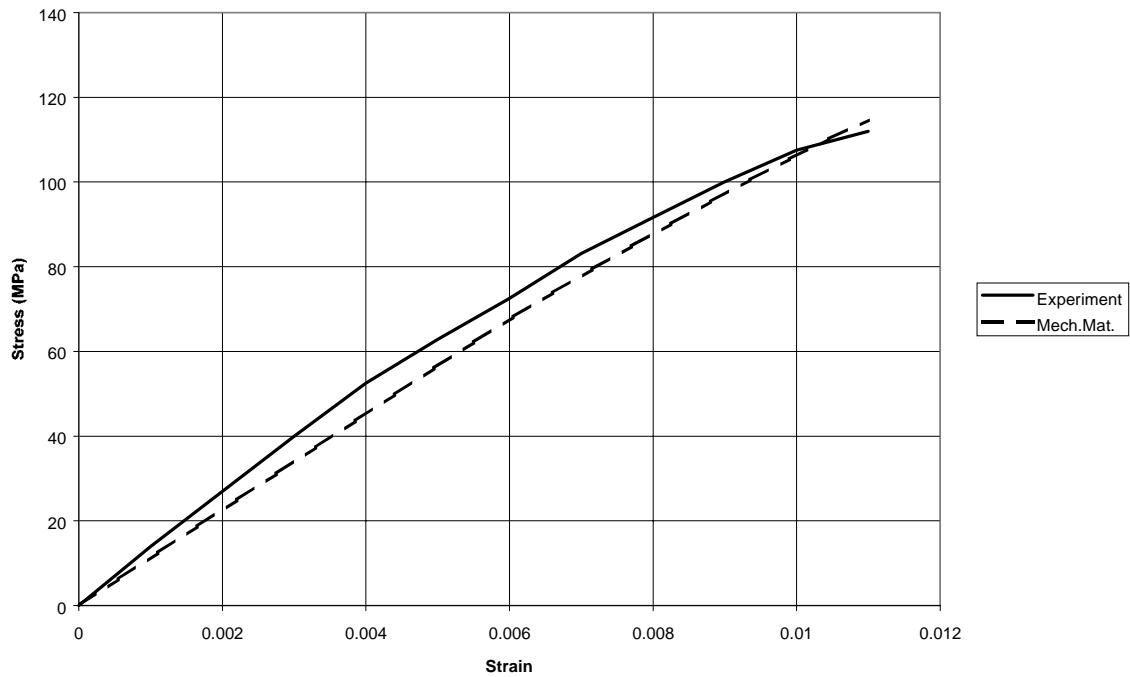
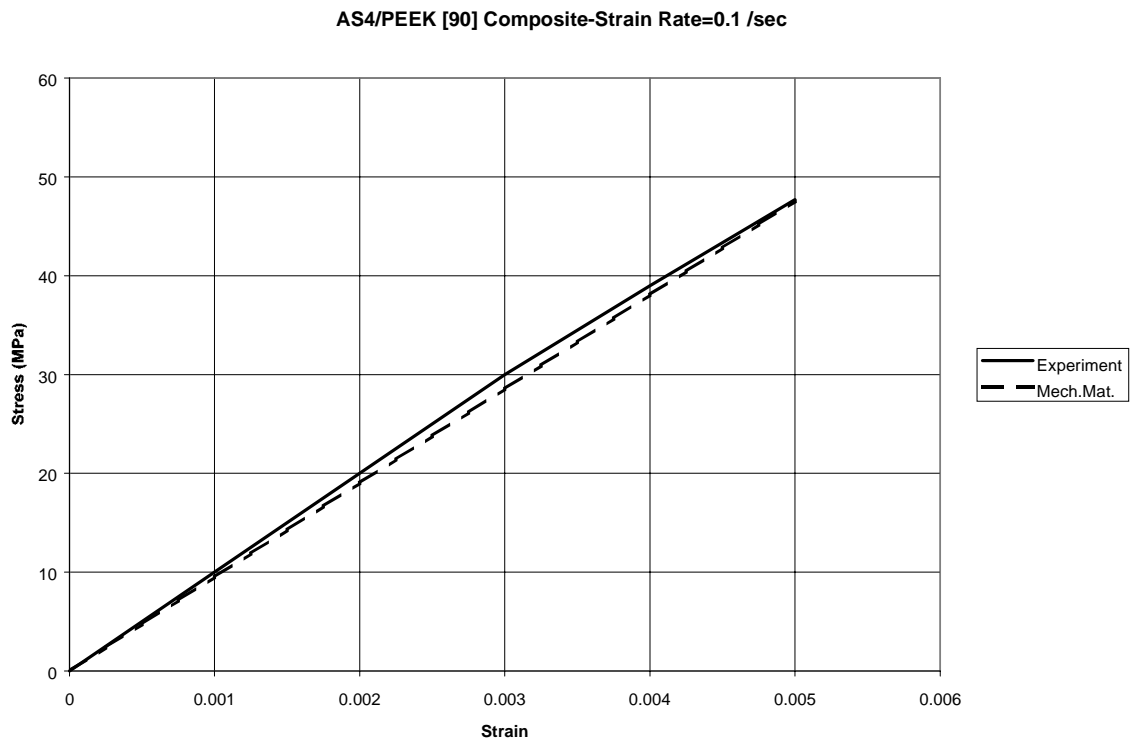
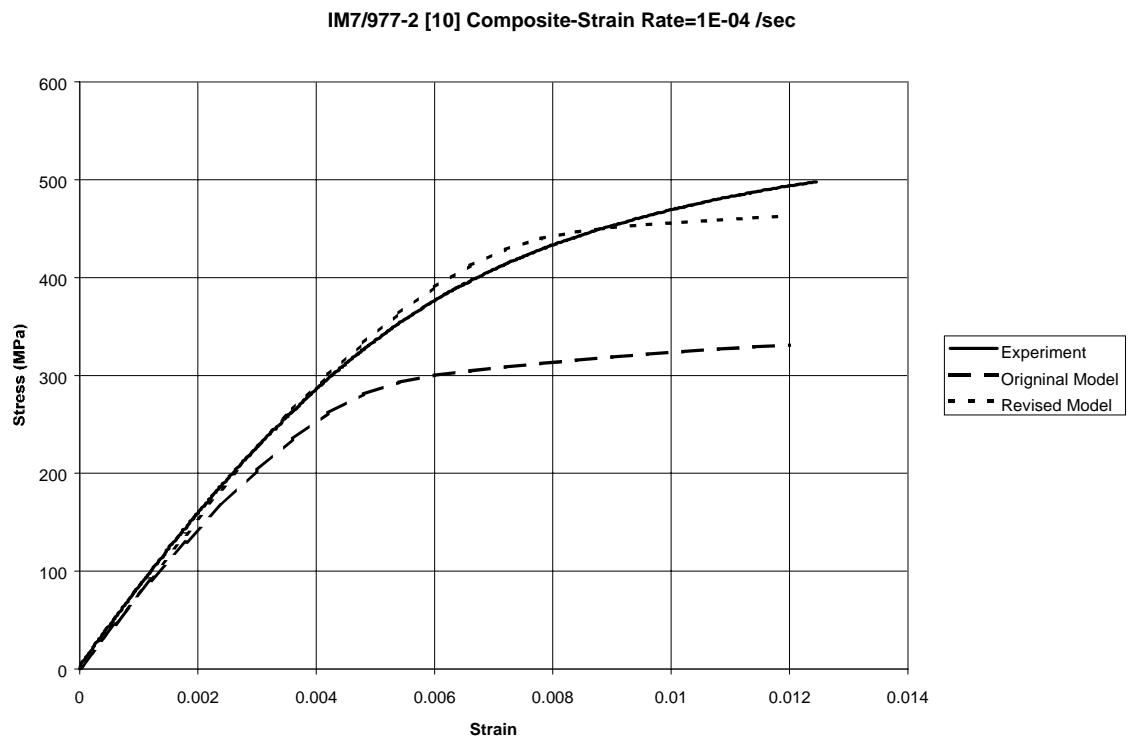


Figure 14: Model Predictions for [45°] AS4/PEEK Laminate with Revised Polymer Model-Strain Rate=0.1 /sec



**Figure 15: Model Predictions for [90°] AS4/PEEK Laminate with Revised Polymer Model-Strain Rate=0.1 /sec**



**Figure 16: Comparison of Results for [10°] IM7/977-2 Laminate Using both Original and Revised Polymer Constitutive Equations**

<b>REPORT DOCUMENTATION PAGE</b>			<i>Form Approved</i> <i>OMB No. 0704-0188</i>	
Public reporting burden for this collection of information is estimated to average 1 hour per response, including the time for reviewing instructions, searching existing data sources, gathering and maintaining the data needed, and completing and reviewing the collection of information. Send comments regarding this burden estimate or any other aspect of this collection of information, including suggestions for reducing this burden, to Washington Headquarters Services, Directorate for Information Operations and Reports, 1215 Jefferson Davis Highway, Suite 1204, Arlington, VA 22202-4302, and to the Office of Management and Budget, Paperwork Reduction Project (0704-0188), Washington, DC 20503.				
<b>1. AGENCY USE ONLY</b> <i>(Leave blank)</i>	<b>2. REPORT DATE</b> March 1999	<b>3. REPORT TYPE AND DATES COVERED</b> Technical Memorandum		
<b>4. TITLE AND SUBTITLE</b> Rate Dependent Deformation and Strength Analysis of Polymer Matrix Composites			<b>5. FUNDING NUMBERS</b>  WU-523-24-13-00	
<b>6. AUTHOR(S)</b>  Robert K. Goldberg and Donald C. Stouffer				
<b>7. PERFORMING ORGANIZATION NAME(S) AND ADDRESS(ES)</b> National Aeronautics and Space Administration John H. Glenn Research Center at Lewis Field Cleveland, Ohio 44135-3191			<b>8. PERFORMING ORGANIZATION REPORT NUMBER</b>  E-11596	
<b>9. SPONSORING/MONITORING AGENCY NAME(S) AND ADDRESS(ES)</b> National Aeronautics and Space Administration Washington, DC 20546-0001			<b>10. SPONSORING/MONITORING AGENCY REPORT NUMBER</b>  NASA TM-1999-209060	
<b>11. SUPPLEMENTARY NOTES</b>  Robert K. Goldberg, Glenn Research Center, Cleveland, Ohio; and Donald C. Stouffer, University of Cincinnati, Cincinnati, Ohio 45221. Responsible person, Robert K. Goldberg, organization code 5920, (216) 433-3330.				
<b>12a. DISTRIBUTION/AVAILABILITY STATEMENT</b>  Unclassified - Unlimited Subject Category: 24  This publication is available from the NASA Center for AeroSpace Information, (301) 621-0390.			<b>12b. DISTRIBUTION CODE</b>  Distribution: Nonstandard	
<b>13. ABSTRACT</b> <i>(Maximum 200 words)</i>  A research program is being undertaken to develop rate dependent deformation and failure models for the analysis of polymer matrix composite materials. In previous work in this program, strain-rate dependent inelastic constitutive equations used to analyze polymers have been implemented into a mechanics of materials based composite micromechanics method. In the current work, modifications to the micromechanics model have been implemented to improve the calculation of the effective inelastic strain. Additionally, modifications to the polymer constitutive model are discussed in which pressure dependence is incorporated into the equations in order to improve the calculation of constituent and composite shear stresses. The Hashin failure criterion is implemented into the analysis method to allow for the calculation of ply level failure stresses. The deformation response and failure stresses for two representative uniaxial polymer matrix composites, IM7/977-2 and AS4-PEEK, are predicted for varying strain rates and fiber orientations. The predicted results compare favorably to experimentally obtained values.				
<b>14. SUBJECT TERMS</b> Composite materials; Impact; Micromechanics; Constitutive equations; Strain rate; Viscoplasticity; Strength			<b>15. NUMBER OF PAGES</b> 36	
			<b>16. PRICE CODE</b> A03	
<b>17. SECURITY CLASSIFICATION OF REPORT</b> Unclassified	<b>18. SECURITY CLASSIFICATION OF THIS PAGE</b> Unclassified	<b>19. SECURITY CLASSIFICATION OF ABSTRACT</b> Unclassified	<b>20. LIMITATION OF ABSTRACT</b>	